

Hybrid and Nonhybrid Lipids Exert Common Effects on Membrane Raft Size and Morphology

Frederick A. Heberle,^{*,†,◆} Milka Doktorova,^{‡,#,◆} Shih Lin Goh,^{‡,◆} Robert F. Standaert,^{†,§,⊥,∇} John Katsaras,^{†,||,∇} and Gerald W. Feigenson^{*,‡}

[†]Biology and Soft Matter and [§]Biosciences Divisions, Oak Ridge National Laboratory, Oak Ridge, Tennessee 37831, United States

[‡]Department of Molecular Biology and Genetics and [#]Tri-Institutional Training Program in Computational Biology and Medicine, Cornell University, Ithaca, New York 14853, United States

[⊥]Departments of Biochemistry and Molecular & Cellular Biology and ^{||}Physics and Astronomy, University of Tennessee, Knoxville, Tennessee 37996, United States

[∇]Joint Institute for Neutron Sciences, Oak Ridge, Tennessee 37831, United States

Supporting Information

ABSTRACT: Nanometer-scale domains in cholesterol-rich model membranes emulate lipid rafts in cell plasma membranes (PMs). The physicochemical mechanisms that maintain a finite, small domain size are, however, not well understood. A special role has been postulated for chain-asymmetric or hybrid lipids having a saturated *sn*-1 chain and an unsaturated *sn*-2 chain. Hybrid lipids generate nanodomains in some model membranes and are also abundant in the PM. It was proposed that they align in a preferred orientation at the boundary of ordered and disordered phases, lowering the interfacial energy and thus reducing domain size. We used small-angle neutron scattering and fluorescence techniques to detect nanoscopic and modulated liquid phase domains in a mixture composed entirely of nonhybrid lipids and cholesterol. Our results are indistinguishable from those obtained previously for mixtures containing hybrid lipids, conclusively showing that hybrid lipids are not required for the formation of nanoscopic liquid domains and strongly implying a common mechanism for the overall control of raft size and morphology. We discuss implications of these findings for theoretical descriptions of nanodomains.

Cell membranes perform multiple functions that may be facilitated by the lateral organization of lipids and proteins into nanoscale compartments, termed membrane rafts.¹ Because of their small size and dynamic nature,² and the chemical complexity of biological membranes, rafts have proven difficult to characterize in cells.³ Three-component mixtures containing a high-melting (high- T_M) lipid, a low-melting (low- T_M) lipid and cholesterol ("HLC" mixtures) are valuable models because they reproduce key properties associated with rafts in animal cell plasma membranes.⁴ Specifically, some HLC mixtures separate into liquid phase domains, reminiscent of the distinct chemical and physical environments central to the raft hypothesis. The study of HLC mixtures offers the possibility of elucidating raft formation at the molecular level by identifying structural aspects of mixture components that influence raft properties, including size and lifetime.³

HLC mixtures yield either nanoscopic or microscopic liquid phase domains, which we previously classified as Type I or II behavior, respectively (Figure S1).⁴ Figure 1 shows three low-

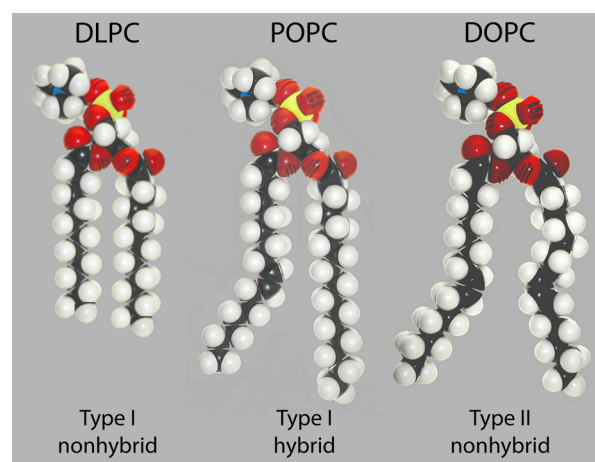


Figure 1. Classification of low-melting lipids.

T_M lipids that generate either Type I or II phase diagrams. Mixtures containing the nonhybrid (i.e., symmetric, having identical acyl chains) lipid 1,2-dioleoyl-*sn*-glycero-3-phosphocholine (DOPC) show liquid-disordered/liquid-ordered (Ld +Lo) phase coexistence of micrometer-sized domains, visible with fluorescence microscopy over a range of composition and temperature (Type II behavior).⁵ In contrast, where the low- T_M component is the hybrid lipid 1-palmitoyl-2-oleoyl-*sn*-glycero-3-phosphocholine (POPC) or 1-stearoyl-2-oleoyl-*sn*-glycero-3-phosphocholine (SOPC), visible domains are absent (Type I behavior).⁶ However, a variety of evidence in POPC- or SOPC-containing HLC mixtures points toward the existence of liquid domains that are smaller than the optical resolution limit of ~ 200 nm.⁷ These observations have inspired a body of theoretical work connecting chain asymmetry to nanodomain

Received: July 24, 2013

formation.⁸ In this model, the more- and less-ordered chains of hybrid lipids located near domain boundaries partition into the ordered and disordered phases, respectively. This preferential alignment is postulated to alleviate interfacial packing frustration, thereby lowering the energetic cost of domain perimeter. A unique “line-active” role for hybrid lipids is an appealing explanation for nanoscopic rafts, as animal cell membranes contain few symmetric low- T_M lipids but an abundance of hybrid lipids.

HLC mixtures containing the nonhybrid, low- T_M lipid 1,2-dilauroyl-*sn*-glycero-3-phosphocholine (DLPC) exhibit Type I behavior.^{6,9} The existence of nanodomains in DLPC-containing mixtures cannot however be explained by the hybrid linactant hypothesis,⁹ raising the intriguing possibility that multiple independent mechanisms control raft size. Such mechanisms can be explored with titration experiments that incrementally replace Type I lipids with Type II lipids, revealing additional details of domain size and morphology transitions that can inform theory.¹⁰ Previously, we found that progressive substitution of the hybrid Type I lipid POPC with the Type II lipid DOPC first increases nanodomain size (as revealed by small-angle neutron scattering, SANS), before inducing modulated phase patterns in a particular range of compositions, and ultimately the large, round domains characteristic of Type II behavior.¹¹ Spatially modulated phases have special significance: they occur when line tension is balanced by competing interactions, e.g., curvature and/or dipole repulsion.¹² Here, we demonstrate an identical domain size and morphology transition for the nonhybrid lipid DLPC. Our observations strongly suggest a common mechanism by which hybrid and nonhybrid lipids reduce line tension.

We examined an HLC mixture containing 1,2-distearoyl-*sn*-glycero-3-phosphocholine (DSPC) as the high- T_M lipid. We generalize our previous notation¹¹ and define $\rho \equiv \chi_{\text{Type II}} / (\chi_{\text{Type I}} + \chi_{\text{Type II}})$ to indicate the fractional replacement of DLPC by DOPC in the mixture. Figure 2 shows representative fluorescence micrographs of giant unilamellar vesicles (GUVs)

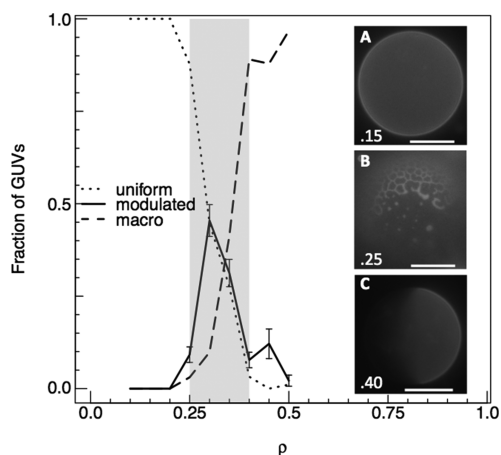


Figure 2. Fluorescence microscopy of GUVs shows a transition from nanoscopic to microscopic domains in a nonhybrid lipid mixture. GUVs exhibited either uniform appearance (A), modulated phase patterns (B), or round domains (C) that depended on the fraction of DOPC [$\rho \equiv \chi_{\text{DOPC}} / (\chi_{\text{DLPC}} + \chi_{\text{DOPC}})$, values shown on images]. The fraction of all GUVs exhibiting these features is plotted vs ρ for the composition DSPC/(DLPC + DOPC)/Chol = 0.35/0.40/0.25. Total GUV counts are enumerated in Table S1. Temperature 23 °C, scale bar 15 μm .

with composition DSPC/(DLPC + DOPC)/Chol = 0.35/0.40/0.25. Three morphological categories were observed: (1) uniform appearance; (2) spatially modulated phase patterns; and (3) large, round domains. The fraction of vesicles exhibiting these morphologies is plotted vs ρ in Figure 2, revealing three distinct compositional regimes: (1) apparently uniform vesicles at $\rho < 0.25$; (2) modulated phases at $0.25 \leq \rho \leq 0.4$; and (3) round domains at $\rho > 0.4$. Similar results were obtained for other compositions within the Ld+Lo coexistence region (Table S2, Figure S2). The domain size and morphology transition is consistent with an increase in line tension as DOPC replaces DLPC. Significantly, the results obtained for this nonhybrid mixture are essentially indistinguishable from previous observations in the hybrid lipid mixture DSPC/(POPC + DOPC)/Chol at similar compositions (Table S4).^{11b,c}

Next, we investigated compositions where GUVs appeared uniform (i.e., $\rho < 0.25$), using techniques sensitive to nanometer length scales. We used Förster resonance energy transfer (FRET) to interrogate domain formation in paucilamellar vesicles (PLVs, vesicles with one to a few lamellae), as previously described.^{7d} Briefly, a sample trajectory that crosses a phase coexistence region (see Figure S1) will exhibit a characteristic pattern of reduced FRET efficiency when fluorescent donor and acceptor lipids partition into different phases. In contrast, a sample trajectory that does not cross a phase boundary (i.e., that remains in a single phase) will exhibit more gradual variation in FRET efficiency due to continuous changes in phase properties (e.g., average molecular area). Figure 3 shows FRET for the nonhybrid mixture DSPC/

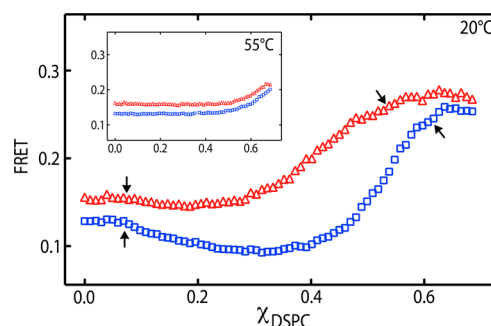


Figure 3. FRET reveals nanodomain formation in a nonhybrid lipid mixture. Sensitized acceptor emission is plotted vs DSPC mole fraction for a sample trajectory (shown in Figure S1) composed of DSPC/(DLPC + DOPC)/Chol, at $\rho = 0$ (red triangles) and 0.25 (blue squares). Plots are offset by 0.02 y-units for clarity. Arrows mark phase boundaries where the trajectory crosses the Ld+Lo coexistence region (see SI for details of boundary determination). Samples between the arrows show reduced FRET efficiency due to partition of DHE donor and BoDIPY-PC acceptor into Lo and Ld phases, respectively. Inset: the same samples measured at 55 °C, revealing gradual changes consistent with uniform mixing.

(DLPC + DOPC)/Chol at $\rho = 0$ and 0.25, for fluorescent donor and acceptor lipids that partition into ordered and disordered phases, respectively. A region of reduced FRET efficiency (RRE) is consistent with coexisting Lo and Ld phases and the resulting segregation of donor and acceptor lipids. The smaller magnitude of the RRE for $\rho = 0$ indicates smaller domains for these compositions.^{7d} We also examined sample trajectories using a disorder-preferring donor and acceptor, which resulted in a characteristic region of enhanced FRET

efficiency due to probe colocalization in Ld domains (Figure S3). In both cases, FRET patterns in nonhybrid mixtures are remarkably similar to those observed in hybrid mixtures of DSPC/(POPC + DOPC)/Chol (Figure S4).^{7d}

Finally, we used small-angle neutron scattering (SANS) to investigate nanoscopic domain formation in 60 nm diameter large unilamellar vesicles (LUVs), using methods described previously.^{11a,13} Briefly, the average scattering length density (SLD) of the aqueous medium and vesicle were matched by adjusting their deuterium content using D₂O and chain-perdeuterated DSPC, respectively (Supporting Information, SI). At the match point, the vesicle and surrounding water have no SLD contrast when lipids are randomly mixed, resulting in no coherent scattering. However, separation of high-melting and low-melting lipids generates in-plane contrast, which produces a scattering signal at length scales corresponding to the domain size. Figure 4 shows scattering intensity vs

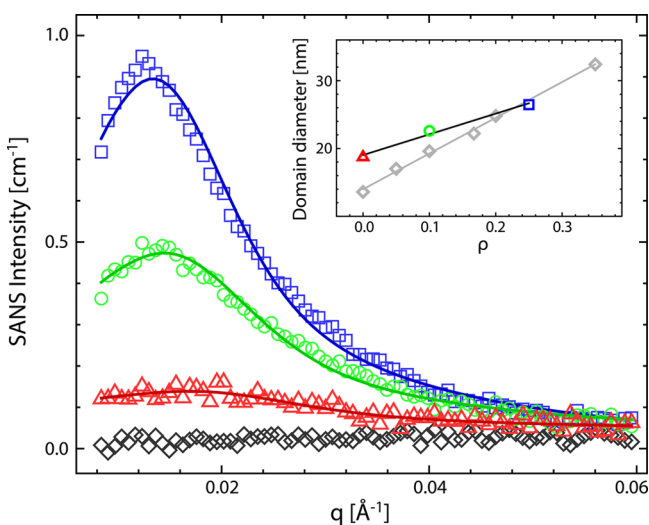


Figure 4. SANS reveals nanodomains in a nonhybrid lipid mixture. SANS intensity vs momentum transfer vector q for LUVs composed of DSPC/(DLPC + DOPC)/Chol = 0.39/0.39/0.22 at 20 °C, for $\rho = 0$ (red triangles), 0.1 (green circles), and 0.25 (blue squares), and a single-phase control sample composed of DSPC/DLPC/Chol = 0.325/0.325/0.35 (black diamonds). Inset: domain size vs ρ determined from Monte Carlo modeling as described in the SI (symbols as before). Also shown are domain sizes for DSPC/(POPC + DOPC)/Chol = 0.39/0.39/0.22 at 20 °C (gray diamonds).^{11a}

momentum transfer vector q for Ld+Lo compositions at $\rho = 0, 0.1, \text{ and } 0.25$ as well as a single-phase control sample. At 20 °C, no scattering is observed in the control sample, whereas increased scattering is observed at $q < 0.06 \text{ \AA}^{-1}$ for the Ld+Lo compositions. Raising the temperature to 55 °C eliminated the scattering in these samples (Figure S5), indicating complete lipid mixing. Domain size was determined using a Monte Carlo analysis (SI) and was found to increase from 18 to 26 nm diameter as ρ increased from 0 to 0.25 at 20 °C (Figure 4 inset, Table S4). The SANS results in these nonhybrid mixtures are qualitatively and quantitatively similar to observations in hybrid mixtures of DSPC/(POPC + DOPC)/Chol.^{11a}

Our results raise questions regarding mechanisms that control the formation and properties of liquid nanodomains in Type I mixtures. Several theories have been advanced to explain nanodomains, including: (1) competing interactions (CI), whereby coexisting liquid (Ld + Lo) phases below the

mixture's critical temperature T_C possess a finite domain size determined by a balance between line tension favoring large domains and an interaction favoring small domains;^{12b,c} (2) Ising-like critical fluctuations (CF) above T_C ;¹⁴ (3) a curvature-induced microemulsion (CM), whereby a structured single phase above T_C arises from coupling between bilayer composition and curvature;¹⁵ and (4) a hybrid-induced microemulsion (HM) above T_C , arising from special behavior of hybrid lipids located near domain interfaces.⁸ Each theory predicts a different mechanism by which Type I lipids reduce liquid domain size. In the case of CI, the contribution of the Type I lipid to mechanical properties of the coexisting phases (e.g., bilayer thickness, bending rigidity, spontaneous curvature, etc.) acts to reduce line tension and/or enhance the competing interaction.^{12b,c} For CF, domains above T_C are described by a correlation length that scales with reduced temperature; the Type I lipid therefore contributes to domain size primarily through its effect on T_C .¹⁴ For CM theory, the important property is the difference in spontaneous curvature between the high- T_M and Type I lipids.¹⁵ Finally, in the case of HM theory, the crucial property is the asymmetric structure of the hybrid lipid's acyl chains.⁸

The observation of composition-dependent nanodomains and modulated phases in both hybrid and nonhybrid mixtures presents new challenges for these theories. Modulated phases are not accounted for by the simple two-dimensional Ising model of CF theory and are predicted by CM theory to have anticorrelated composition across the bilayer midplane,¹⁵ contrary to fluorescence microscopy observations. CI and HM theories each predict correlated modulated phases and nanoscopic domains, yet CI-based simulations might require unphysically large bending moduli to produce modulated phases,^{12c} and HM cannot account for the macroscopic size of modulated phases.^{8f} Furthermore, in HM theory, stripe-like composition fluctuations are a direct consequence of chain asymmetry, specifically the nearest-neighbor interactions of orientationally aligned hybrid lipids located at domain interfaces.^{8f} Given the striking similarities observed here for hybrid and nonhybrid mixtures, we conclude that chain asymmetry is not a unique agent for reducing line tension. However, we cannot exclude the possibility that symmetric lipids located near domain boundaries act via a "hybrid-like" mechanism, whereby nominally identical chains interact differently with adjacent phases to alleviate packing frustration or thickness mismatch. Such interfacial phenomena, as well as contrasts in phase material properties, are likely to play a role in the stabilization of nanoscopic and modulated phases. A unified treatment of the full domain morphology transition observed in four-component mixtures may shed new light on the relative contributions of these or other, as yet unidentified interactions.

We have presented three types of experimental data demonstrating changes in domain size and morphology in HLC mixtures containing only nonhybrid lipids. Comparing our present results with previous results using the hybrid lipid POPC,^{7d,11} we find nanoscopic domains of similar size in both mixtures. Replacing the Type I lipid (DLPC or POPC) with DOPC increases the size of these domains. In both hybrid and nonhybrid four-component mixtures, modulated phase patterns form within a similar composition range, and then transition to large, round domains. These results suggest a common mechanism by which hybrid and nonhybrid Type I lipids reduce line tension. It is therefore reasonable to place DLPC in the category of Type I lipids that includes POPC and SPC:

for these lipids, line tension is sufficiently low that the additional boundary energy associated with multiple small domains is balanced by a competing, repulsive interaction between domains.

■ ASSOCIATED CONTENT

📄 Supporting Information

Figures, tables, and materials and methods. This material is available free of charge via the Internet at <http://pubs.acs.org>.

■ AUTHOR INFORMATION

Corresponding Authors

gwf3@cornell.edu
heberlefa@ornl.gov

Author Contributions

◆ F.A.H., M.D., and S.L.G. contributed equally.

Notes

The authors declare no competing financial interest.

■ ACKNOWLEDGMENTS

We thank Robin Petruzielo for providing supporting data. Support was received from National Science Foundation (NSF) research award MCB 0842839 (to G.W.F.) and from the Laboratory Directed Research and Development Program (to J.K. and R.F.S.) of Oak Ridge National Laboratory (ORNL), managed by UT-Battelle, LLC, for the U.S. Department of Energy (DOE) under contract no. DE-AC05-00OR2275. This work acknowledges support from the Scientific User Facilities Division, Office of Basic Energy Sciences, and the Office of Biological and Environmental Research, DOE, for research conducted at the BioSANS instrument at ORNL's High Flux Isotope Reactor and Center for Structural Molecular Biology. A portion of this research was conducted using the resources of the Cornell Center for Advanced Computing, which receives funding from Cornell University, the NSF, and other leading public agencies, foundations, and corporations.

■ REFERENCES

- (1) (a) Lingwood, D.; Simons, K. *Science* **2010**, *327*, 46. (b) Simons, K.; Gerl, M. J. *Nat. Rev. Mol. Cell Biol.* **2010**, *11*, 688. (c) Simons, K.; Sampaio, J. L. *Cold Spring Harbor Perspect. Biol.* **2011**, *3*, a004697.
- (2) (a) Eggeling, C.; Ringemann, C.; Medda, R.; Schwarzmann, G.; Sandhoff, K.; Polyakova, S.; Belov, V. N.; Hein, B.; von Middendorff, C.; Schönle, A.; Hell, S. W. *Nature* **2009**, *457*, 1159. (b) Sahl, S. J.; Leutenegger, M.; Hilbert, M.; Hell, S. W.; Eggeling, C. *Proc. Natl. Acad. Sci. U.S.A.* **2010**, *107*, 6829.
- (3) Elson, E. L.; Fried, E.; Dolbow, J. E.; Genin, G. M. *Annu. Rev. Biophys.* **2010**, *39*, 207.
- (4) (a) Feigenson, G. W. *Annu. Rev. Biophys. Biomol. Struct.* **2007**, *36*, 63. (b) Feigenson, G. W. *Biochim. Biophys. Acta* **2009**, *1788*, 47.
- (5) (a) Zhao, J.; Wu, J.; Heberle, F. A.; Mills, T. T.; Klawitter, P.; Huang, G.; Costanza, G.; Feigenson, G. W. *Biochim. Biophys. Acta* **2007**, *1768*, 2764. (b) Farkas, E. R.; Webb, W. W. *Rev. Sci. Instrum.* **2010**, *81*, 093704.
- (6) Zhao, J.; Wu, J.; Shao, H.; Kong, F.; Jain, N.; Hunt, G.; Feigenson, G. W. *Biochim. Biophys. Acta* **2007**, *1768*, 2777.
- (7) (a) Silvius, J. *Biophys. J.* **2003**, *85*, 1034. (b) de Almeida, R. F. M.; Loura, L. M. S.; Fedorov, A.; Prieto, M. J. *Mol. Biol.* **2005**, *346*, 1109. (c) Frazier, M. L.; Wright, J. R.; Pokorny, A.; Almeida, P. F. F. *Biophys. J.* **2007**, *92*, 2422. (d) Heberle, F. A.; Wu, J.; Goh, S. L.; Petruzielo, R. S.; Feigenson, G. W. *Biophys. J.* **2010**, *99*, 3309. (e) Petruzielo, R. S.; Heberle, F. A.; Drazba, P.; Katsaras, J.; Feigenson, G. W. *Biochim. Biophys. Acta* **2013**, *1828*, 1302.

- (8) (a) Brewster, R.; Pincus, P. A.; Safran, S. A. *Biophys. J.* **2009**, *97*, 1087. (b) Brewster, R.; Safran, S. A. *Biophys. J.* **2010**, *98*, L21. (c) Yamamoto, T.; Brewster, R.; Safran, S. A. *EPL* **2010**, *91*, 28002. (d) Yamamoto, T.; Safran, S. A. *Soft Matter* **2011**, *7*, 7021. (e) Hirose, Y.; Komura, S.; Andelman, D. *Phys. Rev. E* **2012**, *86*, 021916. (f) Palmieri, B.; Safran, S. A. *Langmuir* **2013**, *29*, 5246.
- (9) Feigenson, G. W.; Buboltz, J. T. *Biophys. J.* **2001**, *80*, 2775.
- (10) Heberle, F. A.; Feigenson, G. W. *Cold Spring Harbor Perspect. Biol.* **2011**, *3*, a004630.
- (11) (a) Heberle, F. A.; Petruzielo, R. S.; Pan, J.; Drazba, P.; Kučerka, N.; Standaert, R. F.; Feigenson, G. W.; Katsaras, J. *J. Am. Chem. Soc.* **2013**, *135*, 6853. (b) Konyakhina, T. M.; Goh, S. L.; Amazon, J. J.; Heberle, F. A.; Wu, J.; Feigenson, G. W. *Biophys. J.* **2011**, *101*, L8. (c) Goh, S. L.; Amazon, J. J.; Feigenson, G. W. *Biophys. J.* **2013**, *104*, 853.
- (12) (a) Baumgart, T.; Hess, S. T.; Webb, W. W. *Nature* **2003**, *425*, 821. (b) Ursell, T. S.; Klug, W. S.; Phillips, R. *Proc. Natl. Acad. Sci. U.S.A.* **2009**, *106*, 13301. (c) Amazon, J. J.; Goh, S. L.; Feigenson, G. W. *Phys. Rev. E* **2013**, *87*, 022708.
- (13) Pan, J.; Heberle, F. A.; Petruzielo, R. S.; Katsaras, J. *Chem. Phys. Lipids* **2013**, *170–171*, 19.
- (14) (a) Veatch, S. L.; Soubias, O.; Keller, S. L.; Gawrisch, K. *Proc. Natl. Acad. Sci. U.S.A.* **2007**, *104*, 17650. (b) Honerkamp-Smith, A. R.; cicuta, P.; Collins, M. D.; Veatch, S. L.; den Nijs, M.; Schick, M.; Keller, S. L. *Biophys. J.* **2008**, *95*, 236. (c) Honerkamp-Smith, A. R.; Veatch, S. L.; Keller, S. L. *Biochim. Biophys. Acta* **2009**, *1788*, 53. (d) Honerkamp-Smith, A. R.; Machta, B. B.; Keller, S. L. *Phys. Rev. Lett.* **2012**, *108*, 265702.
- (15) Schick, M. *Phys. Rev. E* **2012**, *85*, 031902.